

## Thermal plasma decomposition of tetrachloroethylene

Péter Fazekas<sup>1\*</sup>, Zsuzsanna Czégény<sup>1</sup>, János Mink<sup>1</sup>, Pál Tamás Szabó<sup>2</sup>, Anna Mária Keszler<sup>1</sup>,  
Eszter Bódis<sup>1</sup>, Szilvia Klébert<sup>1</sup>, János Szépvölgyi<sup>1</sup>, Zoltán Károly<sup>1</sup>

<sup>1</sup>Institute of Materials and Environmental Chemistry, Research Centre for Natural Sciences,  
Hungarian Academy of Sciences.

Magyar tudósok körútja 2. Budapest, H-1117, Hungary.

<sup>2</sup>MS Metabolomics Laboratory, Core Facility, Research Centre for Natural Sciences,  
Hungarian Academy of Sciences.

Magyar tudósok körútja 2. Budapest, H-1117, Hungary.

\*Corresponding author's e-mail address: [fazekas.peter@ttk.mta.hu](mailto:fazekas.peter@ttk.mta.hu)

Keywords: Tetrachloroethylene, Thermal Decomposition, Radiofrequency Thermal Plasma,  
Waste Management

*(The original article can be found online in the Springer Link database, on the following link:  
<https://link.springer.com/article/10.1007/s11090-018-9895-1>)*

### Abstract

Tetrachloroethylene (C<sub>2</sub>Cl<sub>4</sub>) has been used widely as a solvent and dry cleaning agent, but was later specified as possible human carcinogen. As a result, its safe treatment became a priority. In this paper, we report on its decomposition in an atmospheric radiofrequency

thermal plasma reactor. Main components of the exhaust gases were determined by Fourier transform infrared spectroscopy. We found that complete decomposition can be achieved in either oxidative or reductive conditions but not in neutral one. The solid soot product was characterised by transmission electron microscopy and specific surface area measurement. Organic compounds adsorbed on the surface of the soot were extracted by toluene and comprised, based on gas chromatography mass spectrometry, of various perchlorinated aliphatic (for example hexachlorocyclopentadiene) and aromatic compounds (like hexachlorobenzene, octachloronaphthalene or octachloroacenaphthylene). Several nitrogen containing molecules were also identified whose presence are rare during thermal plasma treatments. Further investigation of the extract by mass spectrometry revealed various higher molar mass chlorinated carbon clusters and two types of fullerenes ( $C_{60}$  and  $C_{70}$ ).

## 1. Introduction

Decomposition of various organic compounds in inductively coupled radiofrequency (RF) thermal plasma was a key research topic in the last two decades. This particular plasma system is characterised by high temperature (8000-12000 K), strong UV radiation and also by very high quenching rate ( $10^6 \text{ K s}^{-1}$ ) [1]. The high plasma temperature and the UV radiation promote the decomposition of processed materials into many reactive species, while their rapid quenching greatly reduces the recombination into large, toxic molecules. Therefore, thermal plasma processing is usually applied in cases when incineration or high-temperature pyrolysis would yield stable, undesired by-products, like soot, dioxins or polycyclic aromatic hydrocarbons (PAHs). Decomposition in thermal plasma has been tested on a large array of compounds, such as (1) small aromatic molecules, like benzene [2], toluene [3] and chlorobenzene [4], (2) linear polymers, like polyethylene [5] and poly(vinyl chloride) [6], (3)

halogenated methane derivatives, like chloroform [7], carbon tetrachloride [8], carbon tetrafluoride [9] and Freon-11 [10] and (4) hydrogen containing C<sub>2</sub> molecules, like dichloroethylene [11]. To best of our knowledge, there have not been reports on the RF thermal plasma decomposition of any hydrogen-free C<sub>2</sub> compounds. For this reason, we selected tetrachloroethylene as a model compound for this work of basic research.

Tetrachloroethylene (C<sub>2</sub>Cl<sub>4</sub>) is a volatile, colourless liquid with a typical sweet odour. It is a non-flammable and highly stable material, which has been used mainly as solvent and cleaning agent for dry cleaning of fabrics. Due to its widespread applications high indoor concentrations up to 124.2 μg m<sup>-3</sup> was measured in Paris [12], and it was even higher (up to 2.9 mg m<sup>-3</sup>) in the close vicinity of dry cleaning facilities [13]. Production of C<sub>2</sub>Cl<sub>4</sub> peaked in the 1970s. Its application has been decreasing after classified as hazardous waste by US Environmental Protection Agency, and as probable human carcinogen (Group 2A) by the International Agency for Research on Cancer (IARC) [14].

In natural conditions C<sub>2</sub>Cl<sub>4</sub> decomposes in vapour phase by reacting with hydroxyl radicals, which is a lengthy process with a half-life of approximately 96 days [15]. In groundwater it is dechlorinated to dichloroethylene and in some cases to ethylene by combined actions of aerobic and anaerobic bacteria [16].

Several papers have dealt with the general thermal degradation of C<sub>2</sub>Cl<sub>4</sub> at high temperatures. Thermal treatment in a quartz tube reactor at temperatures between 310-940 °C in air led to the formation of chlorinated aliphatic carbon molecules, while at higher temperatures the yields of chlorinated cyclopentane/cyclopentenes have been increased [17]. Perchlorinated olefinic (C<sub>3</sub>Cl<sub>6</sub> and C<sub>4</sub>Cl<sub>8</sub>) and aromatic compounds (C<sub>6</sub>Cl<sub>6</sub>, C<sub>8</sub>Cl<sub>8</sub>, C<sub>10</sub>Cl<sub>8</sub>, C<sub>12</sub>Cl<sub>8</sub>) were produced in a flow reactor during pyrolysis in helium at 600-1050 °C [18]. In the presence of excess hydrogen, the number and quantity of chlorinated products decreased

with the temperature. Above 800 °C, the formation of non-chlorinated hydrocarbons (methane, ethane, ethylene, acetylene) was enhanced [19].

In this paper, we report on the decomposition of  $C_2Cl_4$  in an RF thermal plasma system in the absence of auxiliary gases (neutral conditions) and also in the presence of hydrogen (reductive conditions) and oxygen (oxidative conditions). The gas compositions were selected so that results would be comparable with the above cited researches. The gaseous, liquid and solid products were identified by various methods. The addition of hydrogen was of particular interest regarding PAH formation.

## 2. Materials and methods

The RF thermal plasma system used for the decomposition of tetrachloroethylene is shown in Figure 1. The electromagnetic energy with the frequency of 4-5 MHz was produced by a LEPPEL T-30-3-MC-J-TL42 generator and was transferred to a TEKNA PL-35, five-turn-coil plasma torch. The torch was mounted on the double-wall, water cooled, cylindrical stainless steel plasma reactor (121.6 cm length, 19.7 cm inner diameter). The plasma and sheet gases (argon, 99.996 % purity, Linde Gáz Magyarország Ltd.) were flowing through the induction coil with the rate of 15.5 and 29.5 slpm (standard litre per minute), respectively. In particular experiments hydrogen (99.98 %, Linde Gáz Magyarország Ltd.), oxygen (99.5 %, Messer Hungarogáz Ltd.) or helium (99.996 %, Messer Hungarogáz Ltd.) was mixed into the sheet gas to change the reductive/oxidative conditions or the heat transfer properties of the plasma column.  $C_2Cl_4$  (Alfa Aesar, 99 % purity) was fed axially into the plasma flame through an atomizer nozzle (2.16 mm inner diameter) by a Watson Marlow 323 type peristaltic pump. The atomizer gas was also argon with the flow rate of 4.25 slpm.

18 experiments, each of them ten minutes long, were carried out to determine the influence of particular plasma parameters on the decomposition process (Table 1). The plate power

varied between 15 and 25 kW, and the feed rate of the C<sub>2</sub>Cl<sub>4</sub> precursor was in the 260–800 g h<sup>-1</sup> range. The effect of hydrogen and oxygen was examined in stoichiometric gas-C<sub>2</sub>Cl<sub>4</sub> conditions and also with surplus of auxiliary gases. The stoichiometric ratios (SR) were based on the assumption of full reduction (into methane and hydrochloric acid, Eq. 1.) and oxidation (into carbon dioxide and chlorine, Eq. 2.).

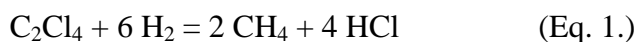


**Table 1.** The experimental conditions of the particular Runs

Run #	Plate power (kW)	Feed rate of C <sub>2</sub> Cl <sub>4</sub> (g h <sup>-1</sup> )	Auxiliary gases		
			Composition	SR	Feed rate (slpm)
Run-1	15	400	—	—	—
Run-2	20	400	—	—	—
Run-3	25	400	—	—	—
Run-4	20	800	—	—	—
Run-5	20	260	—	—	—
Run-6	15	400	H <sub>2</sub>	1	6.1
Run-7	20	400	H <sub>2</sub>	1	6.1
Run-8	25	400	H <sub>2</sub>	1	6.1
Run-9	20	800	H <sub>2</sub>	1	12.2
Run-10	20	260	H <sub>2</sub>	1	4.0
Run-11	20	400	H <sub>2</sub>	2	12.2
Run-12	15	400	O <sub>2</sub>	1	2
Run-13	20	400	O <sub>2</sub>	1	2
Run-14	25	400	O <sub>2</sub>	1	2
Run-15	20	800	O <sub>2</sub>	1	4
Run-16	20	260	O <sub>2</sub>	1	1.2
Run-17	20	400	O <sub>2</sub>	10	20

---

<b>Run-18</b>	20	400	He	25 v%	12.5
---------------	----	-----	----	-------	------

---

The temperature conditions in the plasma were calculated from measurements of optical emission spectroscopy (OES). The emission was collected by a multi-legged fiber-optic cable through a quartz viewport at the height of 70 mm downwards from the bottom turn of the inductive coil and was focused onto a 550 mm monochromator (Jobin-Yvon TRIAX 550), which had a 1200 grooves  $\text{mm}^{-1}$  grating. A charge-coupled device (Jobin-Yvon Spectrum One CCD-3000) was used as the detector with the spectral range of 250-1000 nm and with 0.2 nm resolution. The atomic lines were assigned according to the NIST Atomic Spectral Database [20].

Exhaust gases were sampled at the outlet of the reactor, using a standard, KBr windowed, 10 cm length flow-through gas cell. Fourier transform infrared (FT-IR) spectra were taken in the range of 350-4000  $\text{cm}^{-1}$  by a Varian FTS-7000 spectrometer, equipped with a Peltier-thermostated deuterio triglycine sulphate (DTGS) detector. Every spectrum was based on 64 scans and their resolution was 0.5  $\text{cm}^{-1}$ . Quantitative analysis was done by the integration method using the Quasoft database.

Solid products were collected from the inner surface of the reactor and was characterised by specific surface area measurement (11-point BET isotherm based on nitrogen adsorption at 77 K, Quantachrome Autosorb-1) and transmission electron microscopy (TEM, 100 kV acceleration voltage, Morgagni 268D). In order to understand the chemical composition of the compounds adsorbed on the surface, 10 mg sample from each run were ultrasonically extracted in 1.5  $\text{cm}^3$  toluene (Merck, HPLC grade purity) for 120 minutes then analysed by gas chromatography-mass spectrometry (GC-MS) (Agilent Technologies Inc. 6890 GC/5973 MSD). 1  $\mu\text{l}$  sample was injected to the injector held at 300  $^{\circ}\text{C}$  in splitless mode. The temperature of the GC oven was maintained at 50  $^{\circ}\text{C}$  for 1 minute and then increased to 280  $^{\circ}\text{C}$  at a rate of 10  $^{\circ}\text{C min}^{-1}$ . The volatile products were separated on an Agilent DB-1701

capillary column (30 m length, 0.25 mm inner diameter, 0.25  $\mu\text{m}$  film thickness). The mass spectrometer was operated in electron impact ionisation (EI) mode at 70 eV, in the mass range  $m/z$  14 to 500 Da.

The mass spectrometric measurements were done on a Sciex API2000 tandem mass spectrometer equipped with a heated nebuliser source. Extracts were produced in the same way as for GC-MS measurements and were introduced into the nebuliser by a built-in syringe pump with a flow rate of 150  $\mu\text{l min}^{-1}$ . The source conditions were as follows: curtain gas 35 arbitrary units (AU), source temperature 450  $^{\circ}\text{C}$ , nebulizer current -4  $\mu\text{A}$ , nebulizer gas 30 AU, drying gas 30 AU, declustering potential -20 V. The mass range was 50-1200 Da and scan time was 2 s. Data were acquired in Multi-channel Acquisition (MCA) mode for better sensitivity and isotopic profile. The source temperature was higher as it would be recommended to the flow rate. The reason of this was the absence of higher mass to charge ions at a lower temperature. The elevated temperature helped in ionizing higher number carbon clusters such as fullerenes. The system was purged with toluene after each sample to minimize the cross-contamination.

### 3. Results and discussion

#### 3.1 Thermodynamic calculations

Thermodynamic calculations were performed to predict the species formed after decomposition. The Equilib module of FactSage code, whose goal is to produce the equilibrium composition of given material systems due to the minimization Gibbs energy, was employed in the temperature range of 500-8000 K [21]. Ideal gas conditions were assumed considering the high temperature and almost atmospheric pressure of the plasma system [22].

Three different compositions were examined: (1)  $C_2Cl_4$  without the presence of any auxiliary gases, (2)  $C_2Cl_4 + 6H_2$  (stoichiometric ratio) and (3)  $C_2Cl_4 + 2O_2$  (also stoichiometric ratio).

Based on the thermodynamic calculations, which do not take any kinetical phenomena into consideration, neither composition reaches a fully atomised state even at 8000 K. The  $C_2$  and  $CCl$  radicals are very stable species at high temperatures even in the presence of oxygen; however the later decomposes in reductive environment over 6600 K. Hydrogen tends to form several other stable species as both  $H_2$  and  $HCl$  molecules can be found in the whole temperature range and the  $CH$  radical is present over 2500 K.

Figure 2. illustrates thermodynamic calculation for the  $C_2Cl_4$  system. Simulation (1) predicts a large amount of soot formation in the form of small carbon clusters ( $C_2$ - $C_5$ ). Although according the calculation they disappear below 2500 K, the first condensed phases usually remain in quantity in rapidly quenched plasma systems. Chlorine containing intermediaries, such as  $CCl_2$  and  $C_2Cl_2$  are also present in the 1500-4000 K region, therefore their recombination into  $C_2Cl_4$  is a possibility due to reaction kinetical means.

Figure 3. displays thermodynamic calculation for the  $C_2Cl_4 + 6 H_2$  system. The addition of hydrogen in case (2) creates several small hydrocarbon species ( $CH_2$ ,  $CH_3$ ,  $C_2H$ ,  $C_2H_2$ ,  $C_2HCl$ ), which are expected to recombine into different polyynes ( $C_2H_2$ ,  $C_4H_2$ ,  $C_6H_2$ ,  $C_8H_2$ ) and PAH molecules [6]. The main chlorine molecule becomes  $HCl$ , even temperatures higher than 3000 K, which is favourable to chlorinated hydrocarbons.

Figure 4. shows thermodynamic calculation for the  $C_2Cl_4 + 2 O_2$  system. The equilibrium is the simplest in the presence of oxygen (3). Only atoms, carbon oxides, the  $Cl_2$  molecule and the  $ClO$  intermediate are present below 6000 K, and the later shows a steep decline in concentration under 3000 K. The main products are expected to be  $Cl_2$  and both  $CO$  and  $CO_2$ .

### 3.2 Optical emission spectroscopy and temperature determination

In plasma state different physical and chemical phenomena occur simultaneously. Several temperatures (electron, excitation, rotational, vibrational, etc.) can be defined, which are close to each other in the case of local thermodynamic equilibrium. Determination of these temperatures makes possible to characterise the actual state of plasma. In this study, the excitation temperature of Ar atoms and the vibrational-rotational temperature of two radicals ( $C_2$  and CN) were determined (Runs 2, 7 and 13). In carbon plasmas,  $C_2$  can be almost always detected, while the presence of CN is explained by the nitrogen impurity of the applied gases. A typical emission spectrum is shown in Figure 5.

The excitation temperature was calculated by the Boltzmann plot method using atomic argon lines (Ar I) observed in the wavelength range of 650–1000 nm. This region was chosen because of its absence of molecular bands which was necessary to avoid their overlapping with the spectral lines. Ten Ar I lines were selected on the basis of literature data (at 687.1, 696.5, 703, 714.7, 737.2, 751.4, 794.8, 826.5, 840.8 and 842.5 nm) [23-24]. The most intensive Ar I lines were omitted due to their high tendency for self-absorption. The required physical constants were taken from the NIST Atomic Spectra Database [20]. Standard deviations of the calculated values were  $\pm 10\%$ . Abel inversion was not applied as it is not necessary when the plasma column has a high gradient Gaussian temperature profile as occurs in our plasma system [25].

The excitation temperature of the Ar plasma at particular flow rates and 20 kW plate power was 9000 K. Addition of auxiliary gases increased it above 10000 K. During the plasma treatment of  $C_2Cl_4$  an excitation temperature of 9900 K was measured in neutral conditions. The presence of oxygen did not change the excitation temperature. A similar phenomenon was observed in one of our previous works on the decomposition of chlorobenzene in thermal plasma [4]. In reductive conditions, the excitation temperature increased to 11500 K due to the heating effect of hydrogen (Table 2).

The vibration-rotation temperatures for the C<sub>2</sub> Swan ( $d^3\Pi_g-a^3\Pi_u$  transition, 420-680 nm) and the CN Violet ( $B^2\Sigma-X^2\Sigma$  transition, 350-430 nm) bands were determined by the least-squares fitting code, called Nelder Mead Temperature (NMT), which minimises the difference between the theoretically calculated and the measured emission spectra [26-27]. The calculated temperatures are shown in Table 2. The values are the averages of five simulations and their errors are  $\pm 200$  K. The differences between the vibrational-rotational temperatures of the two radicals refers to certain spatial distributions of the excitation and relaxation of particular chemical species, while the differences between the vibrational-rotational and excitation temperatures prove that the observed part of the plasma column is not in the state of local thermal equilibrium.

**Table 2.** Plasma temperatures during decomposition of C<sub>2</sub>Cl<sub>4</sub>

<b>Run #</b>	<b>Ar excitation T (K)</b>	<b>C<sub>2</sub> Swan T (K)</b>	<b>CN Violet T (K)</b>
<b>Run-2</b>	9900	5870	7940
<b>Run-7</b>	11500	4720	6510
<b>Run-13</b>	9900	no C <sub>2</sub> bands	9500

### 3.3 Analysis of exhaust gases

#### 3.3.1. Qualitative analysis

Gaseous decomposition products of the plasma treatment of C<sub>2</sub>Cl<sub>4</sub> were studied by FT-IR in Run-2 (in Ar), Run-7 (in H<sub>2</sub>) and Run-13 (in O<sub>2</sub>) (Figure 6). The major components of the gas mixture at the reactor outlet were CO, CO<sub>2</sub>, C<sub>2</sub>H<sub>2</sub>, HCN and H<sub>2</sub>O.

CO has one parallel fundamental mode with P- and R-branches with the band origin at  $2143.6 \text{ cm}^{-1}$ . Its presence in neutral and reductive conditions is to be explained by the presence of oxygen traces in the Ar gas.

Four bands of  $\text{CO}_2$  was detected in Run-13, at  $667.6 (v_2)$ ,  $2348.7 (v_3)$ ,  $3616.2 (2v_2 + v_3)$  and  $3714.4 \text{ cm}^{-1} (v_1 + v_3)$ , respectively. The  $v_2$  bending mode exhibits P-, Q- and R-branches as perpendicular vibration. The  $v_3$  antisymmetric  $\text{CO}_2$  stretching has only P- and R-branches which is typical at parallel vibrations. The two combination bands are also parallel modes with only P- and R-branches.

In Run-7 three bands of  $\text{C}_2\text{H}_2$  were identified at  $729.7 (v_5)$ ,  $1326.4 (v_4 + v_5)$  and  $3287.3 (v_3) \text{ cm}^{-1}$ . The  $v_5$  band is the deformational, linear bending mode of the molecule, which exhibits P-, Q- and R-branches (perpendicular band). The  $v_3$  antisymmetric CH stretching is a parallel band exhibiting only P- and R-branches. Beside these two fundamental modes, there is another IR-active, parallel mode band, which is the combination of  $v_4$  and  $v_5$  bands and is detected at  $1326.4 \text{ cm}^{-1}$ . The  $v_4$  linear bending mode is only Raman active at  $611.8 \text{ cm}^{-1}$  therefore it was not observed in this work but its combination with  $v_5$  would give  $1341.5 \text{ cm}^{-1}$  which moves to  $1326.4 \text{ cm}^{-1}$  due to an-harmonic vibrations.

The infrared bands of the HCN molecule were observed at  $712.4 (v_1)$ ,  $1412.4 (v_2)$  and  $3289 (v_3) \text{ cm}^{-1}$  in Run-7. The  $v_1$  band exhibits P-, Q- and R-branches, while  $v_2$  consists of P- and R-branches [28]. It was necessary to subtract the bands of  $\text{C}_2\text{H}_2$  from the spectrum to obtain clearer HCN bands.

Every hitherto discussed molecule has similar band structures with P- and R, or in some cases with P-, Q and R-branches, because they have only one (double degenerate) moment of inertia. However,  $\text{H}_2\text{O}$  is an asymmetric rotor, which has three different moments of inertia, therefore exhibits complicated rotational fine structure. The band origins are obtained by

theoretical analysis and take place at 1594.6 ( $\nu_2$ ), 3656.7 ( $\nu_1$ ) and 3755.8 ( $\nu_3$ )  $\text{cm}^{-1}$  and also as a weak overtone at 3154.4 ( $2\nu_2$ )  $\text{cm}^{-1}$  (Run-7).

Two other compounds were also detected, but their intensities were weak and therefore their concentrations could not have been calculated. Two bands of  $\text{C}_2\text{Cl}_4$  were shown in the spectrum of Run-2 at 795 ( $\nu_{11}$ ) and 918.6 ( $\nu_9$ )  $\text{cm}^{-1}$ , which belongs to the stretching of C-Cl [29]. In Run-13 the band of ONCl was observed at 595.8 ( $\nu_2$ ), 1799 ( $\nu_1$ ) and 2131 ( $\nu_{1+}$   $\nu_3$ )  $\text{cm}^{-1}$  [30]. The presence of HCl was not detected even in reductive atmosphere. This suggests  $\text{Cl}_2$  as the main chlorine molecule in the exhaust gases, even if it is not possible to detect it with the FT-IR technique.

### 3.3.2. Quantitative analysis

The library spectra of the main components, i.e.  $\text{C}_2\text{H}_2$ ,  $\text{H}_2\text{O}$ , HCN, CO and  $\text{CO}_2$  were used for the quantitative analysis. The results obtained by the integration of experimental intensities are summarised in Table 3. Decomposition of  $\text{C}_2\text{Cl}_4$  in neutral condition (Run-2) produced CO ( $60.2 \mu\text{mole dm}^{-3}$ ) and a minor amount of  $\text{C}_2\text{Cl}_4$ . Formation of CO could be attributed to the oxygen traces in the argon while the presence of  $\text{C}_2\text{Cl}_4$  was due to the incomplete decomposition and/or some kind of recombination.

In the presence of hydrogen, the decomposition resulted in smaller amount of CO ( $10.7 \mu\text{mole dm}^{-3}$ ) and some  $\text{H}_2\text{O}$  ( $48.7 \mu\text{mole dm}^{-3}$ ). Hydrogen reacted with C atoms as well, and formed  $\text{C}_2\text{H}_2$  ( $11.1 \mu\text{mole dm}^{-3}$ ) and HCN ( $18.4 \mu\text{mole dm}^{-3}$ ).

**Table 3.** The main gaseous components from  $\text{C}_2\text{Cl}_4$  decomposition

Run #	Component	Band origin frequency ( $\text{cm}^{-1}$ )	Concentration ( $\mu\text{mole dm}^{-3}$ )
Run-2 ( $\text{C}_2\text{Cl}_4$ )	CO	2143.6	60.2

<b>Run-7 (C<sub>2</sub>Cl<sub>4</sub>+H<sub>2</sub>)</b>	CO	2143.6	10.7
	H <sub>2</sub> O	1594.6	48.7
	C <sub>2</sub> H <sub>2</sub>	729.7	11.1
	HCN	712.4	18.4
<b>Run-13 (C<sub>2</sub>Cl<sub>4</sub>+O<sub>2</sub>)</b>	CO <sub>2</sub>	2348.7	153.3

The decomposition process was more complete in the presence of oxygen as compared to neutral and reducing conditions, and it had CO<sub>2</sub> as the main product with some traces of ONCl and H<sub>2</sub>O. Since we did not detect any C<sub>2</sub>Cl<sub>4</sub> in Run-7 or 13 the presence of auxiliary gases seems to be necessary to avoid unwanted recombination of the starting compound.

### 3.4 Analysis of solid products

After each run the solid products consisted of black coloured soot which was collected from the reactor wall. The soot yields were calculated by Eq. 3., and are shown in Table 4:

$$Soot\ yield = \frac{Amount\ of\ soot\ formed\ (g)}{Amount\ of\ carbon\ in\ fed\ tetrachloroethylene\ (g)} \quad (Eq. 3.)$$

In neutral conditions, the soot yield decreased with the plate power (Runs 1, 2 and 3). Increasing the feed rate in the range of 260–800 g h<sup>-1</sup> also increased the soot yield. Similar tendencies were observed in the presence of auxiliary gases, as well, the additions of which, significantly increased gasification and therefore decreased soot formation. Tests with surplus auxiliary gases compared to the 1:1 stoichiometric ratios (Run-11 for H<sub>2</sub> and Run-17 for O<sub>2</sub>) resulted in the highest degree of gasification. The better heat transfer coefficient of helium as compared to argon also led to a lower soot yield than in the case of pure argon (Run-18 vs. Run-2).

**Table 4.** Soot yields of C<sub>2</sub>Cl<sub>4</sub> decomposition

Run #	Condition	Soot yield (%)
Run-1		80
Run-2		76
Run-3	neutral	69
Run-4		80
Run-5		67
Run-6		36
Run-7		31
Run-8	reductive	25
Run-9		35
Run-10		25
Run-11		23
Run-12		22
Run-13		8
Run-14	oxidative	7
Run-15		11
Run-16		6
Run-17		2
Run-18	helium	58

The specific surface area (SSA) of selected soot samples (Table 5) varied in the range of 13 and 40 m<sup>2</sup> g<sup>-1</sup>, which is typical to expandable graphite and graphite foils with the density of 0.3 g cm<sup>-3</sup> [31]. The higher SSA of Run-13 refers to a more porous carbon material which is more similar to carbon black [32].

**Table 5.** Specific surface areas (SSA) of selected soot samples

Run #	SSA (m <sup>2</sup> g <sup>-1</sup> )
-------	---------------------------------------

<b>Run-1</b>	22
<b>Run-2</b>	40
<b>Run-3</b>	13
<b>Run-4</b>	31
<b>Run-5</b>	17
<b>Run-7</b>	24
<b>Run-13</b>	64
<b>Run-18</b>	23

On the TEM micrographs of soot samples produced in neutral conditions typical plate-like particles could be observed (Figure 7-a) with a particle size in the range of 60 to 80 nm. It decreased to 40–60 nm in the presence of hydrogen and increased to 80–120 nm in Ar + O<sub>2</sub> atmosphere (Figure 7-b-c). These values are very similar to the size of carbon particles produced in our previous works [4, 6].

Harbec and co-workers [33-34] reported on the formation of multi-walled carbon nanotubes (MWCNT) during the decomposition of C<sub>2</sub>Cl<sub>4</sub> in DC thermal plasma. In order to establish formation of particular species in our cases we purified some soot samples (Runs 2, 7, 13 and 18) at 500 °C in dry air for two hours [35] to remove the amorphous carbon. However, during treatment samples were completely gasified and thus formation of any crystalline carbon structures could not be confirmed.

### 3.5 Analysis of extracts from soot

#### 3.5.1. Qualitative analysis of organic compounds extracted from the soot

Organic molecules adsorbed on the surface of the solid product were extracted in toluene and were analysed by GC-MS. The identified compounds are listed in Table 6. All of them were aromatic molecules consisting of one or two rings, with the sole exception of the linear

hexachlorobutadiene. We did not detect any oxygen containing molecules. Quite surprisingly, some nitrogen containing molecules were identified (pentachloropyridine, pentachlorobenzonitrile,  $C_9Cl_5N$ ), as well. Although in our recent studies on thermal plasma decomposition of chlorinated compounds OES investigations verified the existence of CN radicals, which referred to the cleavage of the strong  $N\equiv N$  bonds, we could not detect any nitrogen containing species [4, 36]. In this work, however, nitrogen has been incorporated into the extracted products in the ligands and even within the aromatic rings. The absence of nitrogen containing compounds could be explained by the presence of hydrogen in the model compounds (chlorobenzene and PVC): the binding energy of the H–N bonds ( $386 \text{ kJ mole}^{-1}$ ) are lower than any other bonds of hydrogen in the given system (H–C:  $411 \text{ kJ mole}^{-1}$ , H–Cl:  $428 \text{ kJ mole}^{-1}$ , H–H:  $432 \text{ kJ mole}^{-1}$ ), and therefore formation of gaseous species containing H–N bonds was preferred. Nevertheless, it does not explain why we observed the formation of nitrogen-containing compounds in this work even in the case of hydrogen addition (Runs 6-11). Further studies are required to explain this finding.

There are several compounds, which appear in every extracts. Most of them are perchlorinated ones, such as hexachlorobutadiene, pentachloropyridine, pentachlorobenzonitrile, octachloronaphthalene, hexachlorobenzene and octachlorostyrene. This is in perfect agreement with the results of  $C_2Cl_4$  pyrolysis by Tirey [18]. The other reaction products are analogous to hexachlorobenzene and octachlorostyrene, but contain one hydrogen atom, as well (pentachlorobenzene and heptachlorostyrene). It is explained by the presence of  $H_2O$  traces in the  $C_2Cl_4$  and the Ar gas. The above compounds have been formed by the recombination of active fragments of decomposition in the lower temperature region of plasma reactor, even at a high cooling rate of gases.

In neutral conditions, the other products were also perchlorinated ones, excepting two hydrogen containing compounds. We also observed the formation of different chlorinated

cyclopentadiene/cyclopentenes, similarly to C<sub>2</sub>Cl<sub>4</sub> pyrolysis by Yasuhara [17]. The addition of hydrogen and oxygen suppressed the formation of these cyclic molecules. Reductive conditions resulted in the formation of several simple PAH compounds. One monochlorinated compound has been identified (chloronaphthalene), which is in agreement with the literature [37]. Oxygen, which usually has a huge impact on product composition due to its hydrogen removal ability and the consequent perchlorination, had only a small effect due to the absence of hydrogen. In the presence of helium (Run-18) the results were very similar to the neutral conditions. Formation of several isomers of C<sub>9</sub>Cl<sub>5</sub>N and C<sub>8</sub>Cl<sub>6</sub> were observed. However, the cyclopentadiene derivatives disappeared in this case.

In comparison with the existing decomposition methods: traditional pyrolysis yields the same main products [18] while thermal oxidation produces smaller molecules with hexachlorobutadiene as the largest one [17]. The presence of hydrogen is not completely unfolded, because Won did not report on the formation of PAH compounds [19]. However it is worth noting that in these experiments the amount of fed material was rather low, in the order of magnitude of  $\mu\text{l s}^{-1}$ , therefore it is hard to make a perfect comparison.

**Table 6.** Compounds identified in the toluene extracts by GC-MS

Run #	Compounds	Formula	m/z	Ar	H <sub>2</sub>	O <sub>2</sub>	He
1.	Naphthalene	C <sub>10</sub> H <sub>8</sub>	128	–	+	–	–
2.	Chloronaphthalene	C <sub>10</sub> H <sub>7</sub> Cl	162	–	+	–	–
3.	Phanenthrene/anthracene	C <sub>14</sub> H <sub>10</sub>	178	–	+	–	–
4.	Pyrene/Fluoranthene	C <sub>16</sub> H <sub>10</sub>	202	–	+	–	–
5.	Tetrachlorobenzene	C <sub>6</sub> H <sub>2</sub> Cl <sub>4</sub>	216	–	+	–	–
6.	Pentachlorocyclopentadiene	C <sub>5</sub> HCl <sub>5</sub>	236	+	–	–	–
7.	Pentachloropyridine	C <sub>5</sub> NCl <sub>5</sub>	249	+	+	+	+
8.	Pentachlorobenzene	C <sub>6</sub> HCl <sub>5</sub>	250	+	+	+	+
9.	Hexachlorobutadiene	C <sub>4</sub> Cl <sub>6</sub>	258	+	+	+	+
10.	Hexachlorocyclopentadiene	C <sub>5</sub> Cl <sub>6</sub>	270	+	–	–	–

11.	Pentachlorobenzonitrile	C <sub>7</sub> Cl <sub>5</sub> N	273	+	+	+	+
12.	Hexachlorobenzene	C <sub>6</sub> Cl <sub>6</sub>	284	+	+	+	+
13.	C <sub>9</sub> Cl <sub>5</sub> N isomers	C <sub>9</sub> Cl <sub>5</sub> N	297	-	-	-	+
14.	C <sub>8</sub> Cl <sub>6</sub> isomers	C <sub>8</sub> Cl <sub>6</sub>	306	-	-	-	+
15.	Octachlorocyclopentene	C <sub>5</sub> Cl <sub>8</sub>	340	+	-	-	+
16.	Heptachlorostyrene	C <sub>8</sub> HCl <sub>7</sub>	342	+	+	+	+
17.	Heptachloronaphthalene	C <sub>10</sub> HCl <sub>7</sub>	366	+	-	-	+
18.	Octachlorostyrene	C <sub>8</sub> Cl <sub>8</sub>	376	+	+	+	+
19.	Other C <sub>8</sub> Cl <sub>8</sub> isomers	C <sub>8</sub> Cl <sub>8</sub>	376	+	-	-	-
20.	Octachloronaphthalene	C <sub>10</sub> Cl <sub>8</sub>	404	+	+	+	+
21.	Octachloroacenaphthylene	C <sub>12</sub> Cl <sub>8</sub>	424	+	-	-	+
22.	Decachlorobiphenyl	C <sub>12</sub> Cl <sub>10</sub>	494	+	-	-	+

### 3.5.2. Quantitative analysis of organic compounds extracted from the soot

We investigated seven sets of experimental conditions. Four compounds were selected as indicators in all of them, namely C<sub>4</sub>Cl<sub>6</sub>, C<sub>6</sub>Cl<sub>6</sub>, C<sub>8</sub>Cl<sub>8</sub> and C<sub>10</sub>Cl<sub>8</sub>.

The effect of auxiliary gases was compared in Set 1 (Runs 2, 7, 13 and 18) where the plate power (20 kW) and the feed rate (400 g h<sup>-1</sup>) were kept constant. We found that addition of auxiliary gases decreased the formation of indicator molecules in oxidative conditions as compared to neutral ones. The addition of hydrogen reduced the amount of particular compounds, except C<sub>6</sub>Cl<sub>6</sub> (Figure 8-a). The decrease was minor for C<sub>4</sub>Cl<sub>6</sub>, but was significant for C<sub>8</sub>Cl<sub>8</sub> (83%) and C<sub>10</sub>Cl<sub>8</sub> (87%). The still unreacted C and Cl atoms were forming C<sub>6</sub>Cl<sub>6</sub> (23% increase) and carbon was also present in the PAH molecules. In the presence of oxygen, the tendencies were similar (minor decrease in nitrogen containing molecules and a major decrease in the two largest molecules), although the amount of C<sub>4</sub>Cl<sub>6</sub> increased by 51%. The C<sub>6</sub>Cl<sub>6</sub> concentration was increased by 34%. The addition of helium decreased the amount of the primary product (C<sub>6</sub>Cl<sub>6</sub>). The C<sub>4</sub>Cl<sub>6</sub> and C<sub>8</sub>Cl<sub>8</sub> also decreased while the amount of C<sub>10</sub>Cl<sub>8</sub> did not change at all.

The effect of plate power and feed rate were investigated for the pure argon case in Sets 2 and 3. The increase of plate power from 15 to 25 kW (Set 2, Runs 1-3) increased the energy content of the plasma column, which resulted in lower concentrations of  $C_4Cl_6$ ,  $C_6Cl_6$  and  $C_{10}Cl_8$ . At the same time a minor increase of  $C_8Cl_8$  was observed. The higher energy content of the plasma flame seems to be favourable for the construction of ligand-containing perchlorinated molecules (Figure 8-b). In Set 3 (Runs 2, 4 and 5) the higher feed rates led to higher concentrations of every indicator molecules. It is explained by the lower specific energy of the plasma system (i. e. plate power divided by feed rate), which resulted in a different thermal story of the products of decomposition (Figure 8-c).

In the remaining sets the effects of plate power and feed rate were compared in the presence of hydrogen and oxygen, respectively. In reductive conditions, the increase of plate power (Set 4, Runs 6-8) resulted in decreased concentration of  $C_6Cl_6$  (8.6% at 20 kW and 14.3 % at 25 kW) and an increase by two orders of magnitude of the other indicator molecules. The increase of plate power from 15 to 25 kW led to the following increased yields:  $C_4Cl_6$  by 470%,  $C_8Cl_8$  by 337% and  $C_{10}Cl_8$  by 348% (Figure 8-d). Higher feed rates resulted in increased concentrations (Set 5, Runs 7, 9 and 10) (Figure 8-e).

In the presence of oxygen, the increased plate power resulted in a decrease in every indicator except for  $C_8Cl_8$  (Set 6, Runs 12-14) (Figure 8-f). A tenfold oxygen excess significantly depressed soot formation. However, it had only a small effect on the formation of adsorbed organic compounds. Higher feed rates similarly to Sets 3 and 5 resulted in increased concentrations (Set 7, Runs 13, 15 and 16) (Figure 8-g).

### 3.6 Toxicity of the reaction products

$C_2Cl_4$  itself has an oral medial lethal dose (LD50) of 2600 mg  $kg^{-1}$  for rats and more than 5000 mg  $kg^{-1}$  for mice. No deaths were reported at the level of 4000 mg  $kg^{-1}$  in cats and dogs,

and at 5000 mg kg<sup>-1</sup> in rabbits. In humans only the 500 mg kg<sup>-1</sup> dose was investigated and was proven nonfatal.

The four indicator compounds show different toxic behaviours. Hexachlorobenzene is very similar to C<sub>2</sub>Cl<sub>4</sub> since its oral LD50 values are in the 1700-4000 mg kg<sup>-1</sup> range for various species, although continuous exposure causes acute neurological toxicity, like tremor, incoordination and weakness. Humans do not suffer from these symptoms, and hexachlorobenzene behaves only as skin irritant. Octachloronaphthalene was tested on turkeys: 125 mg kg<sup>-1</sup> day<sup>-1</sup> dose was mixed in their food and was found to have no effect on them where 100 mg kg<sup>-1</sup> day<sup>-1</sup> hexachloronaphthalene killed all test animals. Octachlorostyrene was investigated on Sprague Dawley rats in 500 mg kg<sup>-1</sup> concentration which caused liver hypertrophy. The most toxic of the four molecules is hexachlorobutadiene. Its oral LD50 is between 90 and 350 mg kg<sup>-1</sup> in various species of mice, rats and guinea pigs. Vineyard workers, who were exposed to 0.8-3 mg m<sup>-3</sup> concentration in fumigated areas, exhibited multiple toxic effects like disturbance of nervous functions, hypotension and cardiac disease.

The decomposition products in the presence of hydrogen contained some PAH molecules as well. Naphthalene has an oral LD50 value of 354-2400 mg kg<sup>-1</sup> in rats and its lethal dose in humans are around 319-574 mg kg<sup>-1</sup> based on suicides attempted by mothballs. Phenanthrene has lower oral LD50 in rats (700 mg kg<sup>-1</sup>) but its isomer, anthracene, has a value three order of magnitude higher (160000 mg kg<sup>-1</sup>). Pyrene's is also high, 2700 mg kg<sup>-1</sup>. All of them cause the photosensitization of skin of humans.

From toxicological point of view it is recommended to use auxiliary gases during the plasma decomposition to decrease the amount of by-products. It is also preferable to exclude the use of hydrogen to avoid the formation of unwanted PAH compounds. The presence of oxygen also removes the chlorinated cyclopentene and cyclopentadiene derivatives [15].

### 3.7 Analysis of extracts by mass spectrometry

During extractions for GC-MS measurements, the colourless toluene solvent turned into yellow or even reddish-brown in several cases. This phenomenon is an indicator of the formation of fullerene molecules. Therefore, further MS investigations were made to verify their presence. The results are shown in Table 7.

We could observe both buckminsterfullerene ( $C_{60}$ ) and  $C_{70}$  molecules in the extracts prepared from the solid decomposition products in neutral (Runs 1-5), reductive (Runs 6-11) conditions, and in the presence of helium (Run-18), as well (Figure 9). We also detected their oxidised derivatives, such as  $C_{60}O$  and  $C_{70}O$ . Although recent research in a specialised plasma system yielded higher fullerenes from  $C_{74}$  to  $C_{98}$  [38], they could not have been observed in this work.

Several chlorinated carbon clusters (CCC) were also detected. They belonged to two groups, the  $C_xCl_8$  and  $C_yCl_{10}$  series, where “x” and “y” are even numbers, which are always rising by two within the series. This is comparable to the results of the decomposition of  $CCl_4$  in arc plasma, where “x” ranged from 10 to 14 and “y” from 16 to 28 [39]. It also refers to the inclusion of  $C_2$  species into the next cluster, which is supported by the presence of intensive  $C_2$  Swan bands in the optical emission spectra. The mass spectra showed some CCCs with impurities too.

**Table 7.** Compounds identified in the toluene extracts by mass spectrometry

No.	Formula	m/z
1.	$C_{60}$	720
2.	$C_{70}$	840
3.	$C_{60}O$	736
4.	$C_{70}O$	856

<b>5.</b>	$C_{12}Cl_8$	424
<b>6.</b>	$C_{14}Cl_8$	448
<b>7.</b>	$C_{14}Cl_{10}$	518
<b>8.</b>	$C_{16}Cl_{10}$	542
<b>9.</b>	$C_{18}Cl_{10}$	566
<b>10.</b>	$C_{20}Cl_{10}$	590
<b>11.</b>	$C_{22}Cl_{10}$	614
<b>12.</b>	$C_6Cl_5O$	263
<b>13.</b>	$C_8Cl_7O$	357
<b>14.</b>	$C_{10}Cl_7O$	381
<b>15.</b>	$C_{12}Cl_7O$	405
<b>16.</b>	$C_5NOCl_4$	230
<b>17.</b>	$C_7NOCl_4$	254

#### 4. Conclusions

In this paper we used  $C_2Cl_4$  as a model molecule to gain better understanding of the thermal plasma treatment of perchlorinated, linear hydrocarbons. We employed several analytical methods to describe the plasma column and the various decomposition products. In neutral conditions we found small amount of unreacted or recombined  $C_2Cl_4$  in the exhaust gases, while the presence of auxiliary gases made the decomposition complete. Additionally, they increased gasification and reduced the amount of solid soot products. According to electron micrographs the soot consisted of 40-120 nm large, plate-like particles resembling to carbonaceous material of expanding graphite having alike specific surface area.

Extraction of adsorbed molecules from the soot surface revealed several perchlorinated cyclic compounds. Their amount was reduced by both the increase of plate power and the presence of oxygen or hydrogen. The beneficial effect of the latter is overshadowed by the simultaneous formation of several types of PAHs. Further analysis of the extracts by mass spectrometry also revealed the formation of fullerenes ( $C_{60}$  and  $C_{70}$ ) and several chlorinated carbon clusters.

The RF thermal plasma system is a suitable tool for the decomposition of the perchlorinated  $C_2Cl_4$  model compound and is a commercially available method for this task, although due to its large maintenance cost its application could be economical only, when large amount of waste must be treated.

Acknowledgements: The authors are grateful to Miklós Prodán and Gábor Babos for their technical assistance. Furthermore, we would like to thank Csaba Németh and Péter Németh for their contribution to the FT-IR and TEM measurements, respectively.

## References

1. Boulos, M., Fauchais, P., Pfender, E. (1994): Thermal Plasmas: Fundamentals and applications. Plenum Press, New York.
2. Shih, S.-I., Lin, T-C., Shih, M. (2004): Decomposition of benzene in the RF plasma environment, Part I. Formation of gaseous products and carbon depositions. Journal of Hazardous Materials 116 239-248.
3. Föglein, K. A., Babievskaya, I., Szabó, P. T., Szépvölgyi, J. (2003b): Recent studies on the decomposition of n-hexane and toluene in RF thermal plasma. - Plasma Chemistry and Plasma Processing 23 233-243.
4. Fazekas, P., Bódis, E., Keszler, A. M., Czégény, Zs., Klébert, Sz., Károly, Z., Szépvölgyi, J. (2013): Decomposition of chlorobenzene by thermal plasma processing. Plasma Chemistry and Plasma Processing 33 765-778.
5. Gudetti, R. R., Knight, R., Grossmann, E. D. (2000): Depolymerization of polyethylene using induction-coupled plasma technology. Plasma Chemistry and Plasma Processing 20 37-64.

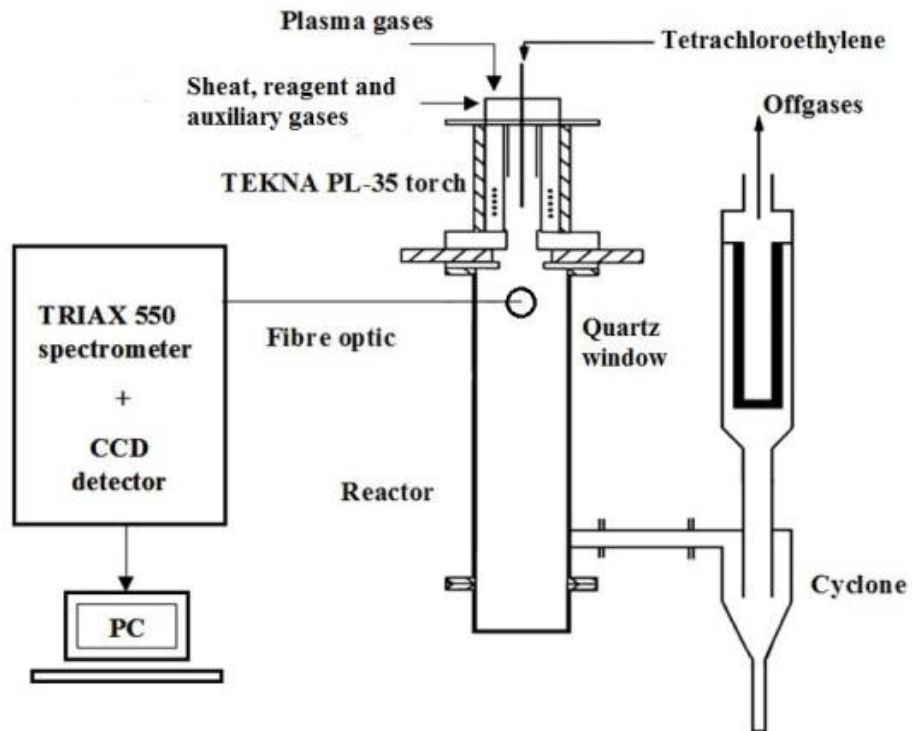
6. Fazekas, P., Czégény, Zs., Mink, J., Bódis, E., Klébert, Sz., Németh, Cs., Keszler, A. M., Károly, Z., Szépvölgyi, J. (2016): Decomposition of poly(vinyl chloride) in inductively coupled radiofrequency thermal plasma. *Chemical Engineering Journal* 302 163-171.
7. Föglein, K. A., Szabó, P. T., Babievskaya, I. Z., Szépvölgyi, J. (2005b): Comparative study on the decomposition of chloroform in thermal and cold plasma. *Plasma Chemistry and Plasma Processing* 25 289-301.
8. Föglein, K. A., Szabó, P. T., Dombi, A., Szépvölgyi, J. (2003a): Comparative study of the decomposition of  $\text{CCl}_4$  in cold and thermal plasma. *Plasma Chemistry and Plasma Processing* 23 651-664.
9. Sun, J.-W., Park, D.-W. (2003):  $\text{CF}_4$  decomposition by thermal plasma processing. *Korean Journal of Chemical Engineering* 20 476-481.
10. Föglein, K. A., Szépvölgyi, J., Szabó, P. T., Mészáros, E., Pekker-Jakab, E., Babievskaya, I. Z., Mohai, I., Károly, Z. (2005a): Comparative study on decomposition of  $\text{CFCl}_3$  in thermal and cold plasma. *Plasma Chemistry and Plasma Processing* 25 275-288.
11. Lee, W-J., Chen, C-Y., Lin, W-C., Wang, Y-T., Chin, C-J. (1996): Phosgene formation from the decomposition of 1,1- $\text{C}_2\text{H}_2\text{Cl}_2$  contained gas in an RF plasma reactor. *Journal of Hazardous Materials* 48 51-67.
12. Roda, C., Kousignian, I., Ramond, A., Momas, I. (2013): Indoor tetrachloroethylene levels and determinants in Paris dwellings. *Environmental Research* 120 1-6.
13. Chiappini, L., Delery, L., Leoz-Garziandia, E., Brouard, B., Fagault, Y. (2009): A first French assessment of population exposure to tetrachloroethylene from small dry cleaning facilities. *Indoor Air* 19 226-233.

14. WHO (World Health Organization) (2010): Tetrachloroethylene. WHO Guidelines for indoor air quality: selected pollutants. 415-454.
15. Wexler, P. (2014): Encyclopedia of toxicology, third edition (Editor-in-chief). Elsevier.
16. Chang, C-H., Yang, H-Y., Hung, J-M., Lu, C-J., Liu, M-H. (2017): Simulation of combined anaerobic/aerobic bioremediation of tetrachloroethylene in groundwater by a column system. *International Biodeterioration & Biodegradation* 117 150-157.
17. Yasuhara, A. (1993): Thermal decomposition of tetrachloroethylene. *Chemosphere* 26 1507-1512.
18. Tirey, D. A., Taylor, P. H., Kasner, J., Dellinger, B. (1990): Gas phase formation of chlorinated aromatic compounds from the pyrolysis of tetrachloroethylene. *Combustion Science and Technology* 74 137-157.
19. Won, Y-S. (2009): Thermal decomposition of tetrachloroethylene with excess hydrogen. *Journal of Industrial and Engineering Chemistry* 15 510-515.
20. Kramida, A., Ralchenko, Y., Reader J. (2016): NIST Atomic Spectra Database (Version 5.4). – National Institute of Standards and Technology, Gaithersburg, Maryland, 20899-8320. <http://physics.nist.gov/asd>.
21. FactSage 2016: Bale, C. W., Bélisle, E., Chartrand, P., Decterov, S. A., Eriksson, G., Gheribi, A. E., Hack, K., Jung, I-H., Kang, Y.-B., Melançon, J., Pelton, A. D., Petersen, S., Robelin, C., Sangster, J., Spencer, P., Van Ende, M-A. (2016): FactSage thermochemical software and databases 2010-2016. *Calphad* 54 35-53.
22. Cota-Sanchez, G., Soucy, G., Huczko, A., Lange, H. (2005): Induction plasma synthesis of fullerenes and nanotubes using carbon black-nickel particles. *Carbon* 43 3153-3166.

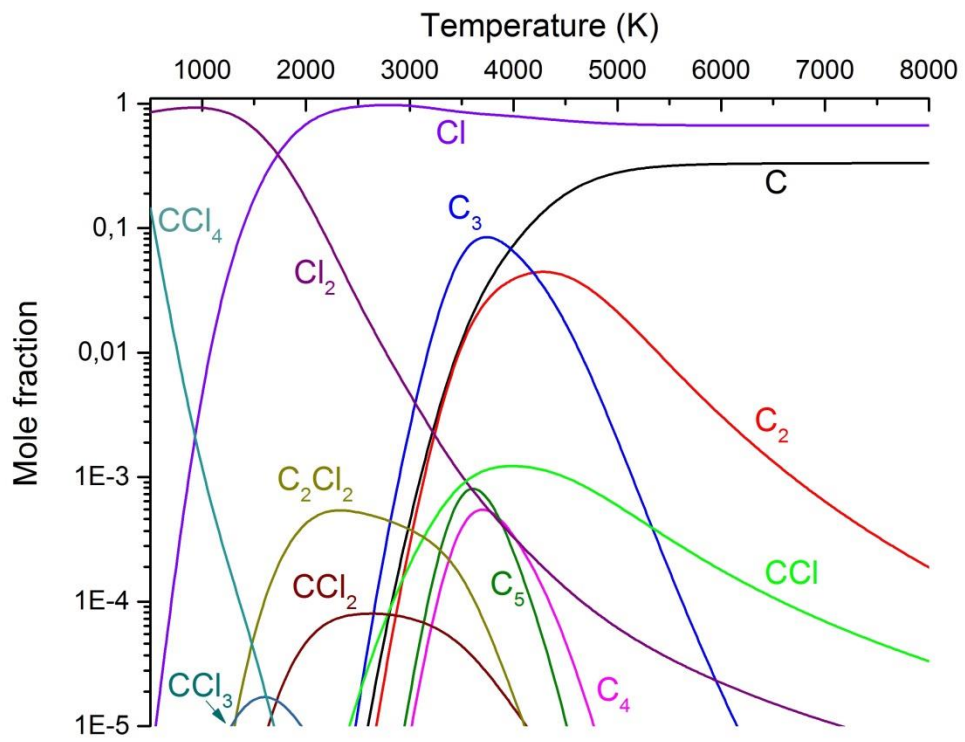
23. Jamroz, P., Zyrnicki, W. (2010): Optical emission spectroscopy study for nitrogen-acetylene-argon and nitrogen-acetylene-helium 100 kHz and DC discharges. *Vacuum* 84 940-946.
24. Yugeswaran, S., Selvaranjan, V. (2006): Electron number density measurements on a DC argon plasma jet by stark broadening of Ar I spectral line. *Vacuum* 81 347-352.
25. Bussiere, W., Vacher, D., Menecier, S., André, P. (2011): Comparative study of an argon plasma and an argon copper plasma produced by an ICP torch at atmospheric pressure based on spectroscopic methods, *Plasma Sources Science and Technology* 20 1-23.
26. Hornkohl, J. O., Parigger, C. G., Lewis, J. W. L. (1991): Temperature measurements from CN spectra in a laser induced plasma. *Journal of Quantitative Spectroscopy & Radiative Transfer* 46 405-411.
27. Parigger, C. G., Plemmons, D. H., Hornkohl, J. O., Lewis, J. W. L. (1994): Spectroscopic temperature measurements in a decaying laser-induced plasma using the C<sub>2</sub> Swan system. *Journal of Quantitative Spectroscopy & Radiative Transfer* 52 707-711.
28. Choi, K. N., Barker, E. F. (1932): Infrared absorption spectrum of hydrogen cyanide. *Physical Review* 42 777-785.
29. Mann, D. E., Acquista, N., Plyer, E. K. (1954): Vibrational spectra of tetraflouroethylene and tetrachloroethylene. *Journal of Research of the National Bureau of Standards* 52 67-72.
30. Jones, L. H., Ryan, R. R., Asprey, L. B. (1968): Vibrational spectra and force constants for isotopic species of nitrosyl chloride. *The Journal of Chemical Physics* 49 581-585.

31. Shornikova, O. N., Kogan, E. V., Sorokina, N. E., Avdeev, V. V. (2009): The specific surface area and porous structure of graphite materials. *Russian Journal Physical Chemistry A* 83 1022-1025.
32. Rodat, S., Abanades, S., Grivei, E., Patrianakos, G., Zygoianni, A., Konstandopoulos, A. G., Flamant, G. (2011): Characterization of carbon black produced by solar thermal dissociation methane. *Carbon* 49 3084-3091.
33. Harbec, D., Meunier, J-L., Guo, L., Gauvin, R., El Mallah, N. (2004): Carbon nanotubes from the dissociation of  $C_2Cl_4$  using a dc thermal plasma torch. *Journal of Physics D: Applied Physics* 37 2121-2126.
34. Harbec D., Meunier, J-L., Gou, L., Jureidini, J. (2007): A parametric study of carbon nanotubes production from tetrachloroethylene using a supersonic thermal plasma jet. *Carbon* 45 2054-2064.
35. Colomer, J-F., Piedigrosso, P., Willems, I., Journet, C., Bernier, P., Van Tendeloo, G., Fonseca, A., Nagy, J. B. (1998): Purification of catalytically produced multi-walled nanotubes. *Journal of the Chemical Society, Faraday Transactions* 94 3753-3758.
36. Fazekas, P., Keszler, A. M., Bódis, E., Drotár, E., Klébert, Sz., Károly, Z., Szépvölgyi, J. (2015): Optical emission spectra analysis of thermal plasma treatment of poly(vinyl chloride). *Open Chemistry* 13 549-556.
37. Eiceman, G. A., Hoffman, R. V., Collins, M. C., Long, Y-T., Lu, M-Q. (1990): Chlorine substitution reactions of polycyclic aromatic hydrocarbons on fly ash from coal-fired power plants. *Chemosphere* 21 35-41.
38. Alexakis, T., Tsantrizos, P. G., Tsantrizos, Y. S., Meunier, L-S. (1997): Synthesis of fullerenes via the thermal dissociation of hydrocarbons. *Applied Physics Letters* 70 2102-2104.

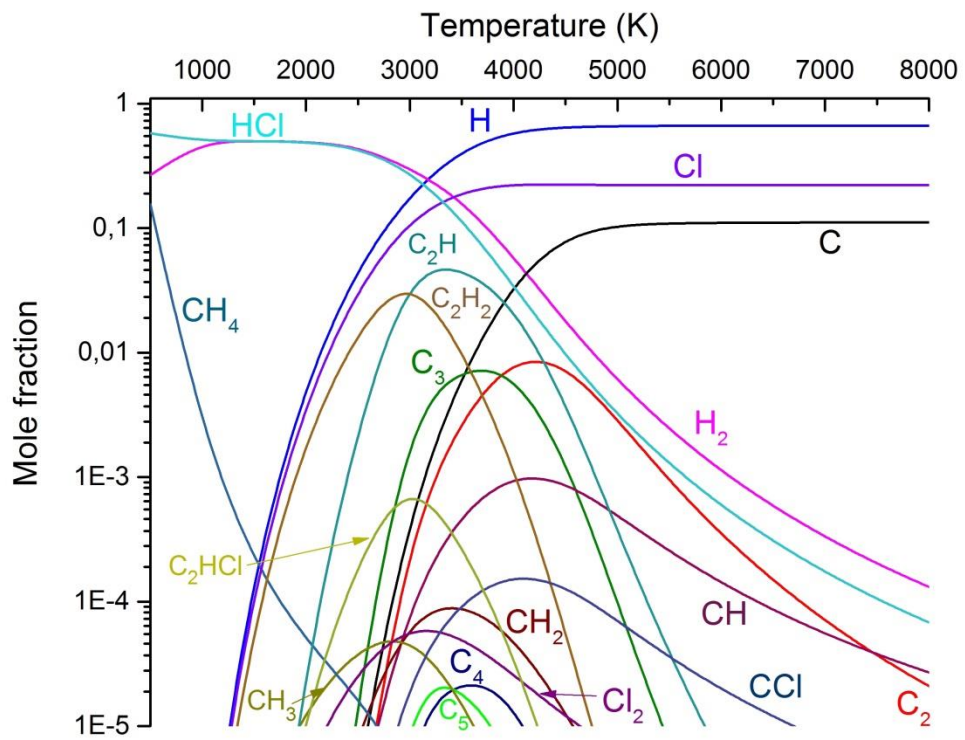
39. Gao, F., Xie, S-Y., Ma, Z-J., Feng, Y-Q., Huang, R-B., Zheng, L-S. (2004): The graphite arc-discharge in the presence of  $\text{CCl}_4$ : Chlorinated carbon clusters in relation with fullerenes formation. *Carbon* 42 1959-1963.



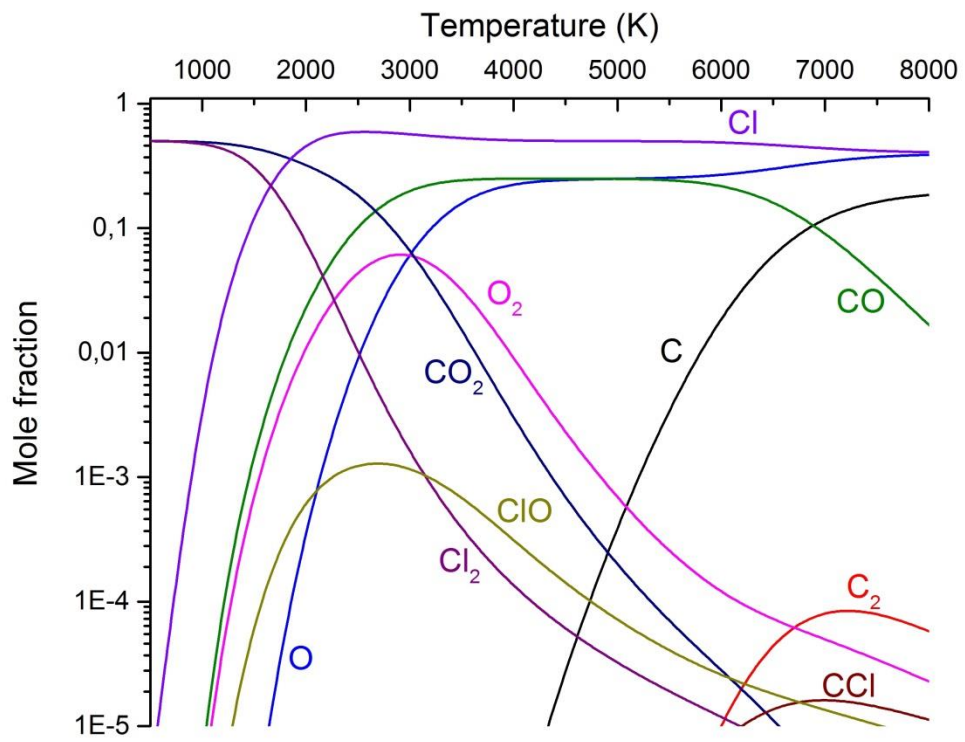
**Figure 1.** Scheme of the plasma reactor



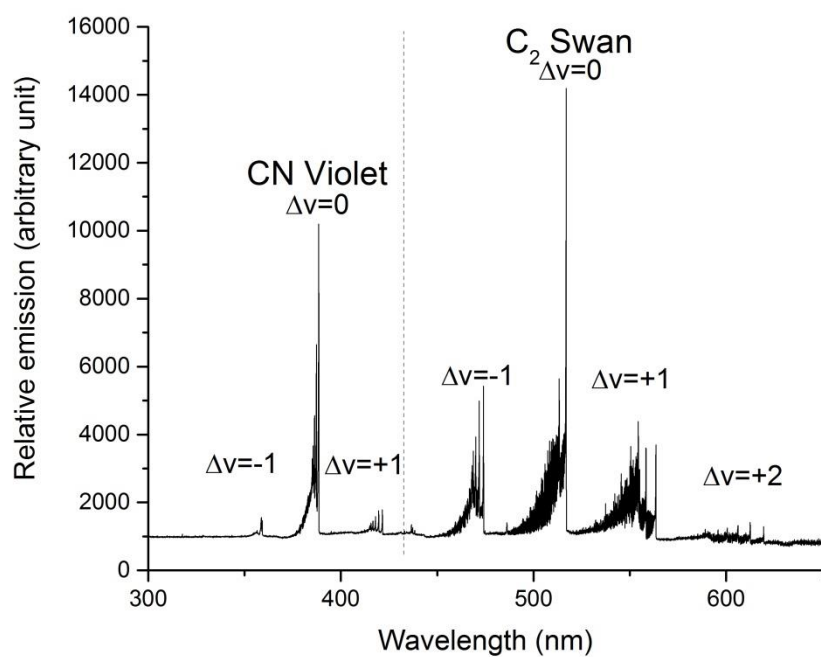
**Figure 2.** Thermodynamic calculation for the  $C_2Cl_4$  system (1)



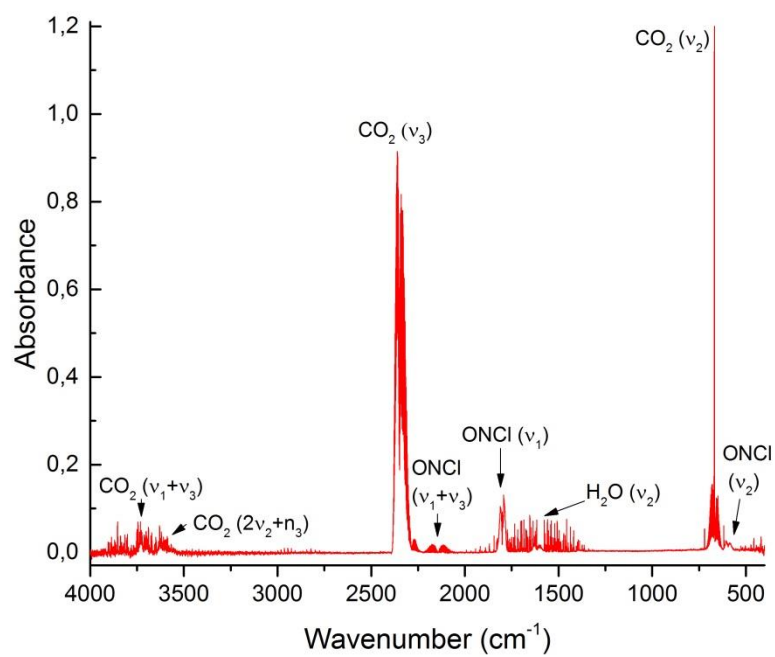
**Figure 3.** Thermodynamic calculation for the  $C_2Cl_4 + 6H_2$  system (2)



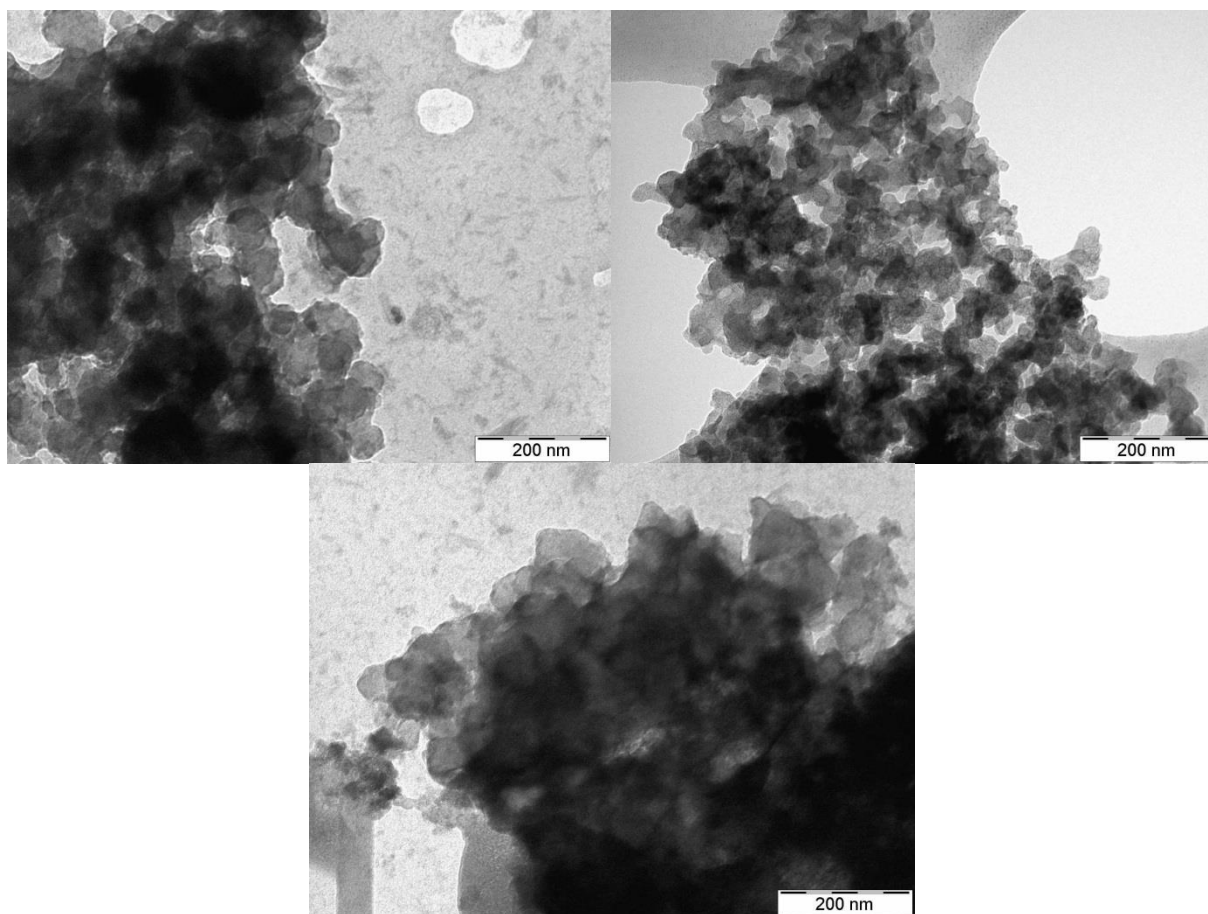
**Figure 4.** Thermodynamic calculation for the  $C_2Cl_4 + 2O_2$  system (3)



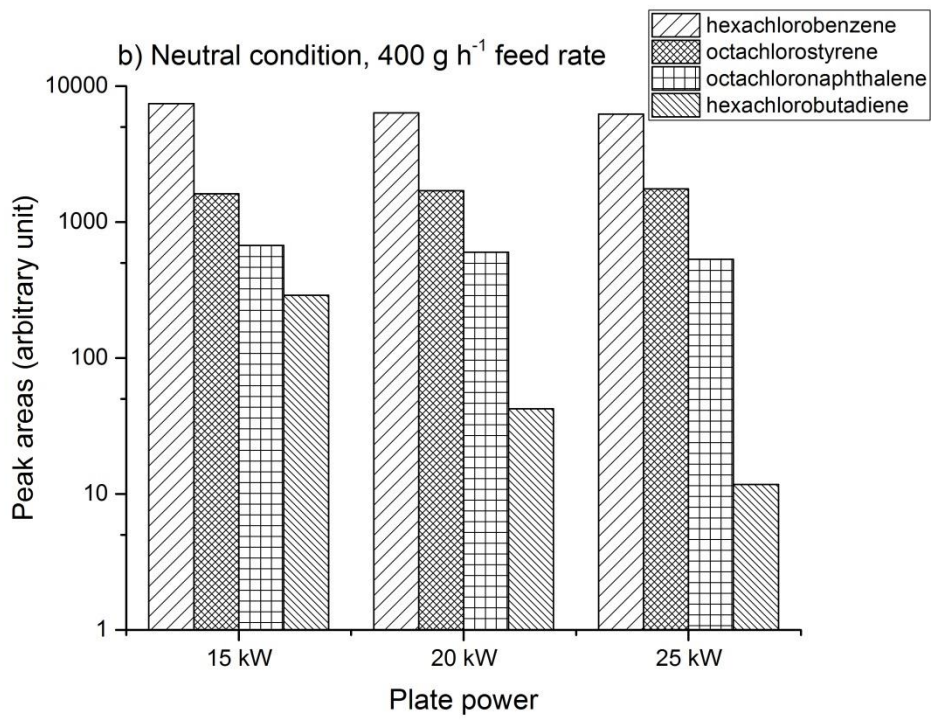
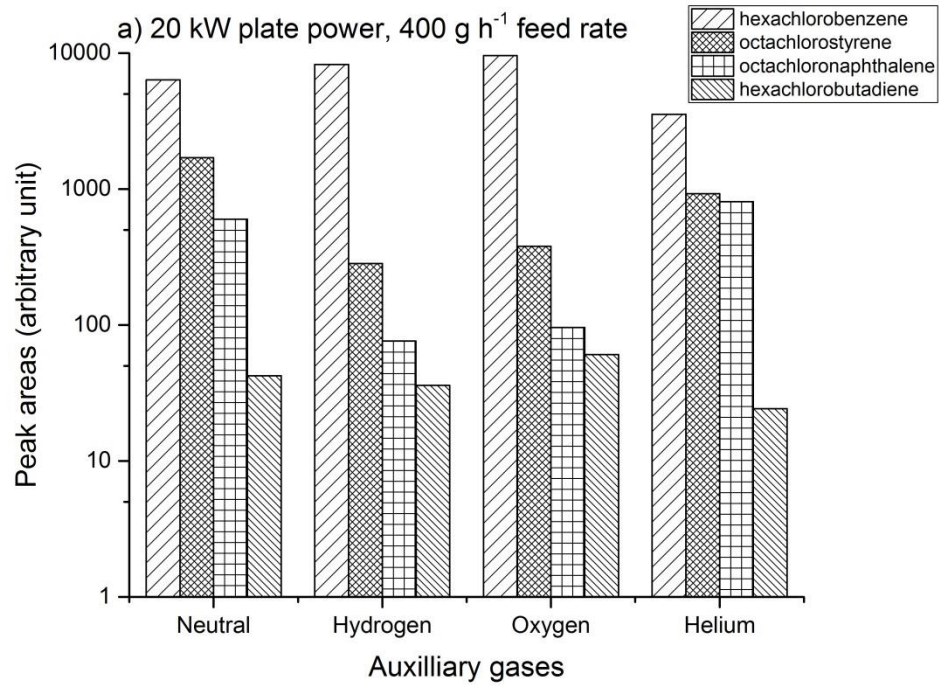
**Figure 5.** CN Violet and C<sub>2</sub> Swan bands in the optical emission spectrum of Run-7

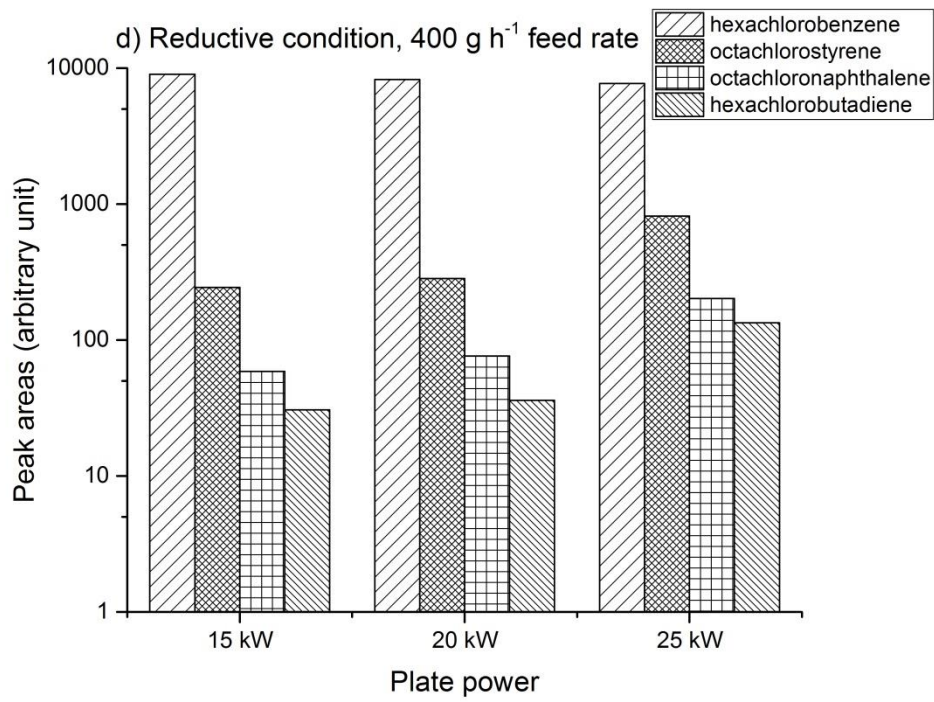
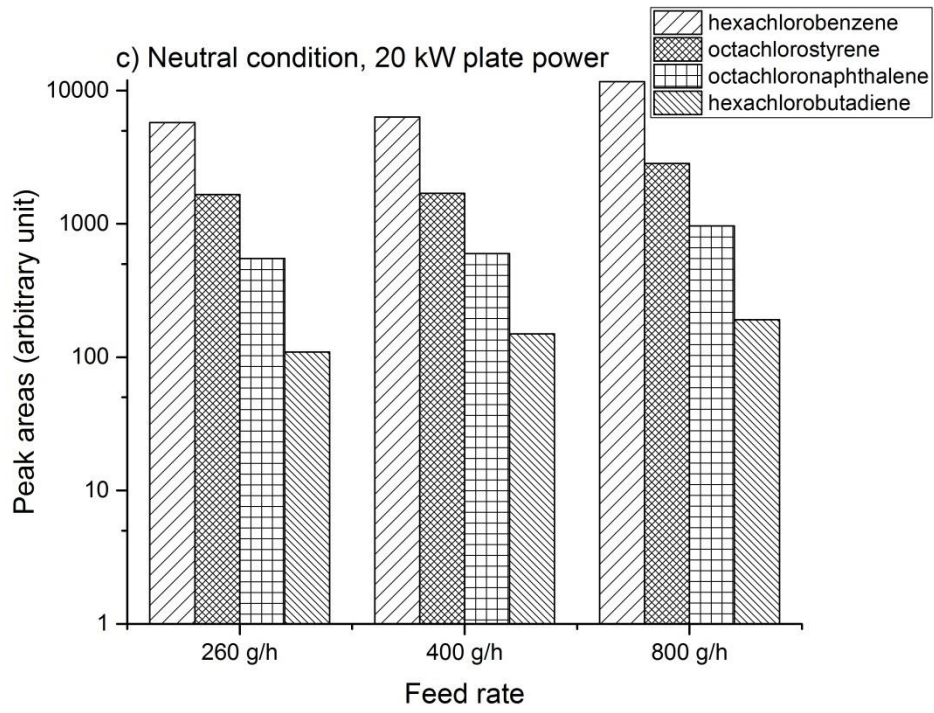


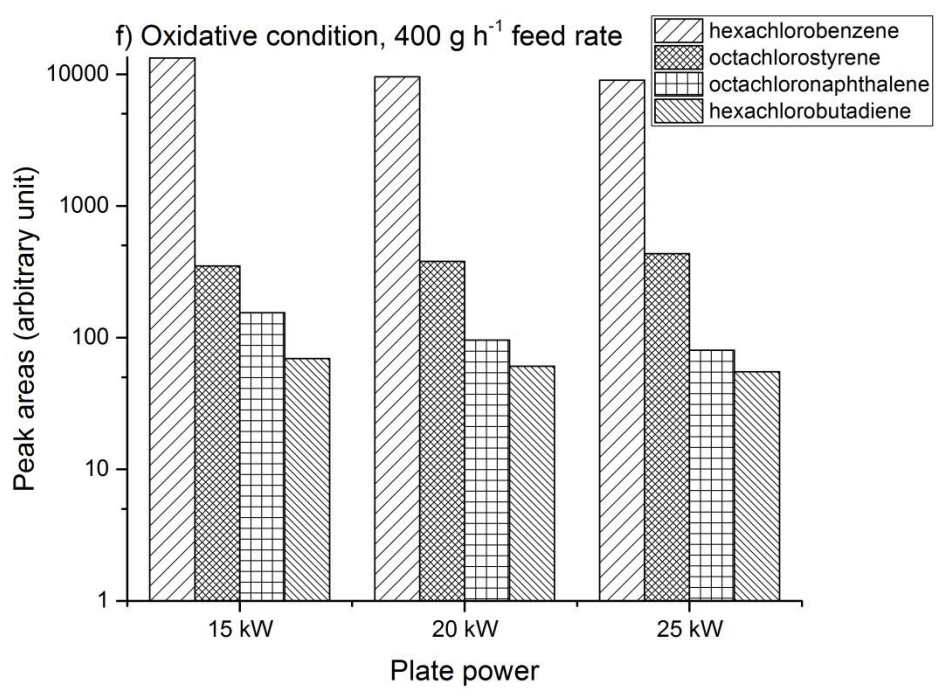
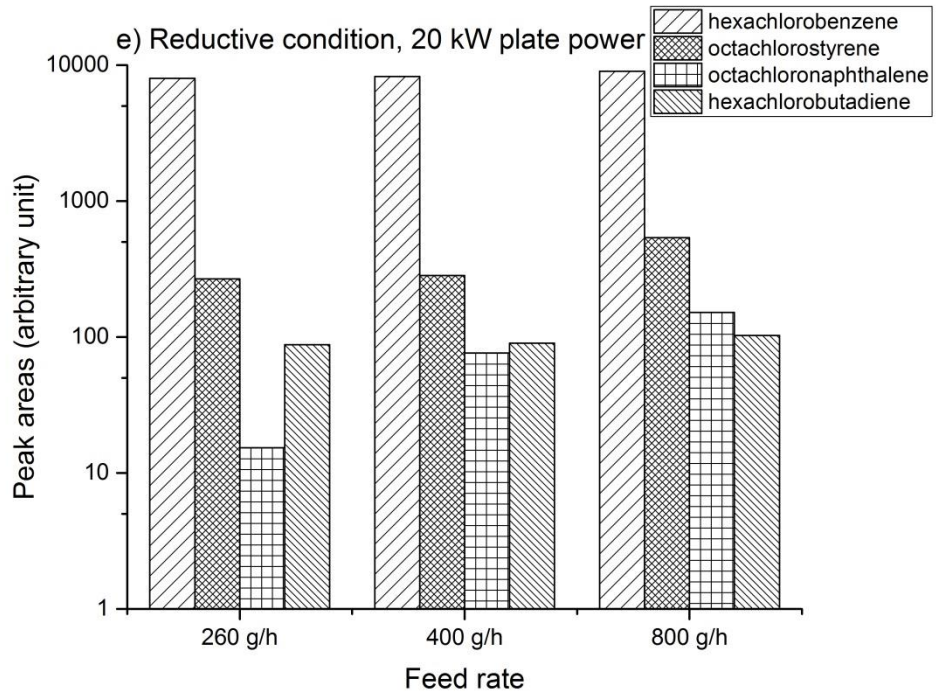
**Figure 6.** Composition of gaseous products in Run-13



**Figure 7.** Soot morphology obtained (a) in neutral condition (Run-2), (b) in reductive condition (Run-7) and (c) in oxidative condition (Run-13)







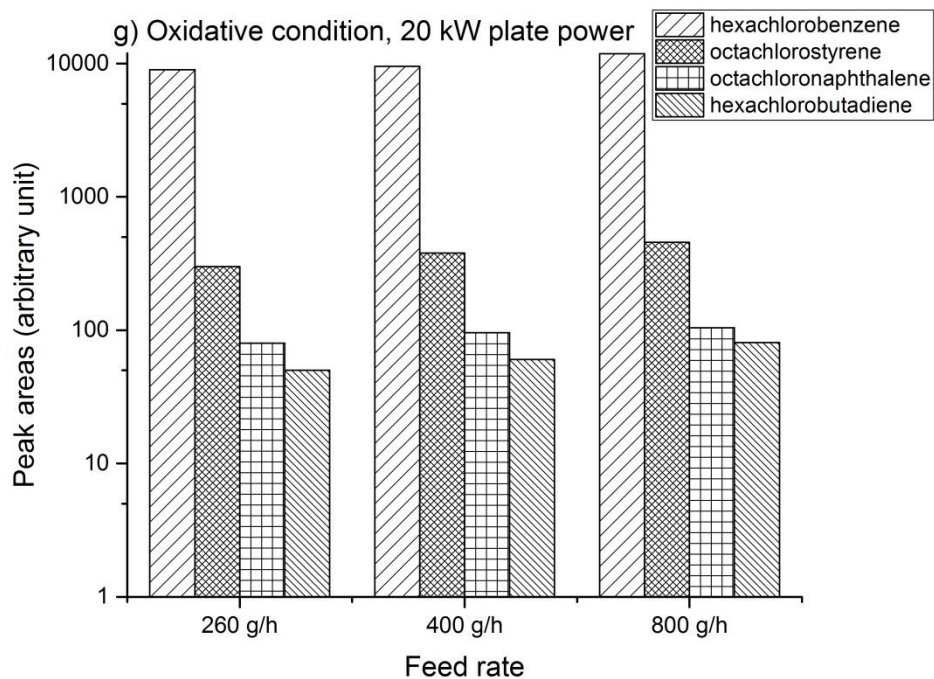


**Figure 8. (a-g).** Effect of experimental conditions on the formation of perchlorinated compounds: (a) gas composition (b) plate power under neutral conditions, (c) feed rate under neutral conditions, (d) plate power in the presence of hydrogen, (e) feed rate under reductive conditions, (f) plate power in the presence of oxygen, (g) feed rate under oxidative conditions

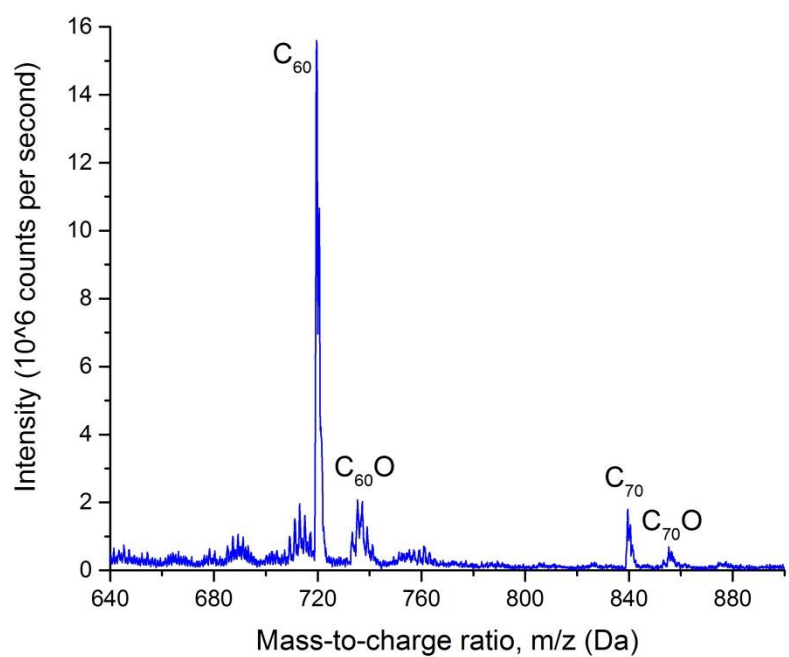


**Figure 9.** C<sub>60</sub> and C<sub>70</sub> molecules in the mass spectrum of Run-18